Walker breakdown of Brownian domain wall dynamics

Markus Weißenhofer,* Severin Selzer, and Ulrich Nowak
Fachbereich Physik, Universität Konstanz, DE-78457 Konstanz, Germany

(Received 13 July 2022; revised 19 August 2022; accepted 12 September 2022; published 26 September 2022)

The Brownian motion of domain walls in uniaxial and biaxial ferromagnetic nanowires is studied, comparing spin dynamics simulations with analytical calculations within the framework of a collective coordinate approach. Our results demonstrate that the interplay between spatial and angular dynamics gives rise to a complex time dependence of the MSD in biaxial nanowires and to a drastically reduced diffusion coefficient in uniaxial nanowires, analogous to magnetic skyrmions. This diffusion suppression is also responsible for the peculiar temperature dependence of the diffusion coefficient in biaxial systems: while it is found to scale linearly with temperature up to a certain threshold, the emergence of a *Walker breakdown of Brownian motion* is responsible for a reduction of the diffusion coefficient with increasing temperature above this threshold.

DOI: 10.1103/PhysRevB.106.104428

I. INTRODUCTION

The motion of topologically protected textures in magnetically ordered materials has been the subject of intense research over the last decades owing to its potential for promising recording and processing technologies for magnetically stored information, e.g., via their usage in a racetrack memory [1,2]. Most of the effort has been focused on their unidirectional motion induced by external driving forces. It has been demonstrated that they can be moved using electric currents [3–8] and temperature gradients [9–11].

For domain walls (DWs), experimental investigations have revealed that their field-driven motion is ultimately hindered by a drastic slowing down for higher fields [12]. This phenomenon is the so-called *Walker breakdown*, which had already been predicted by Schryer and Walker [13] in the 1970s based on an effective, one-dimensional model for the DW dynamics in biaxial nanowires. The emergence of a Walker breakdown in nanowires is fundamentally linked to the coupling between the spatial and angular dynamics of DWs and the presence of a broken rotational symmetry in the plane perpendicular to the easy axis [14,15]. Due to the coupling between the spatial and angular dynamics, a moving DW is tilted from the equilibrium angle. As long as the fields are low, the restoring force due to the angular potential induced by the broken rotational symmetry balances this tilt and the DW moves with constant velocity. However, above a critical field (the *Walker field* [13]) the DW can overcome the potential energy barrier and the constant motion gives way to an oscillating motion, which leads to a considerable decrease in the DW velocity. In a similar fashion, a Walker breakdown emerges for the current-driven dynamics [16,17] and the temperature-gradient-driven dynamics of DWs [18–20].

While the deterministic motion of DWs has been investigated in numerous theoretical and experimental studies, the impact of thermal fluctuations on their dynamics has attracted less attention. It was shown that thermal fluctuations play a key role in the depinning behavior of DWs driven by fields [21] and currents [22]. Purely thermal motion, i.e., their thermal diffusion (Brownian motion), has been studied based on an effective quasiparticle description considering only spatial dynamics [23–25], using micromagnetic simulations for nanowires with high perpendicular anisotropy [26] and spin dynamics simulations for chiral DWs in ultrathin films [27]. This lack of studies on DW diffusion can be explained by the fact that in experimental situations the diffusive motion of DWs tends to be suppressed by pinning. However, recent progress in the fabrication of ultralow-pinning materials, which also lead to the experimental demonstration of Brownian motion of magnetic skyrmions [28], might render the diffusion of DWs relevant, possibly even obstructing their potential application in proposed magnetic recording and processing devices. Instead, the emergence of DW diffusion might also fuel the proposal of novel, nonconventional computing devices exploiting the stochastic nature of Brownian motion, in analogy to what has been proposed for magnetic skyrmions [28–31]. Henceforth, we conclude that more thorough investigations of DW diffusion are needed in order to gain a deeper understanding of its fundamentals, possibly paving the way for its efficient control and manipulation.

Here we study the Brownian motion of DWs in uniaxial and biaxial ferromagnetic nanowires. First, we derive expressions for the sMSD and the diffusion coefficients based on the description of DW dynamics within a collective coordinate approach, taking into account both the spatial and angular dynamics. As such, this goes beyond what is done in Ref. [27], where the authors considered an effective description for only the spatial dynamics of DWs. Then we compare the analytical formulas with results from spin dynamics simulations based on the stochastic LLG equation for an atomistic spin model. The interplay between spatial and angular dynamics of the DWs gives rise to a drastically reduced diffusion coefficient in uniaxial nanowires as compared to biaxial nanowires.

*markus.weissenhofer@uni-konstanz.de

In addition, we find a peculiar dependence of the diffusion coefficient in biaxial systems on temperature: while it is found to scale linearly with temperature up to a certain threshold temperature, the emergence of a *Walker breakdown of Brownian motion* is responsible for a reduction of the diffusion coefficient with increasing temperature above this threshold. Our calculations suggest that this novel type of Walker breakdown also occurs in systems where the rotational symmetry is broken by other means, such as a perpendicularly applied magnetic field or a Dzyaloshinsky-Moriya interaction (DMI) [32,33].

II. THEORY

In this section we discuss the Brownian motion of ferromagnetic DWs within a one-dimensional continuum model using a collective coordinate approach. We start by deriving coupled Langevin-type effective equations of motion for the two relevant degrees of freedom, the DW position Z and DW angle Ψ, from a Lagrangian approach. Subsequently, we use these coupled stochastic differential equations (SDEs) to calculate the mean squared displacements (MSDs) and the diffusion coefficients of DWs in uniaxial (easy axis along the nanowire) and biaxial nanowires (additional intermediate axis perpendicular to the nanowire).

A. Derivation of effective Langevin-type equations of motion

It is well established to describe the motion of DWs within a one-dimensional continuum model [15], where the discrete spins are replaced by a continuous vector field via $\boldsymbol{S}_i \to \boldsymbol{S}(z)$. Here, without loss of generality, the system is assumed to be extended in z direction. By introducing spherical variables $\Theta(z)$ and $\Phi(z)$, the spatial dependence of the spin vector field can be expressed as $\boldsymbol{S}(z) = (\cos\Phi(z)\sin\Theta(z), \sin\Phi(z)\sin\Theta(z), \cos\Theta(z))^{\mathrm{T}}$. For the sake of readability, the dependence on z is omitted hereinafter. The Lagrangian and the Rayleigh dissipation functional describing ferromagnetic dynamics are given by [34]

$$L[\Theta,\Phi] = -\int \left(\frac{\mathcal{M}}{\gamma}\dot{\Phi}\cos\Theta\right) dz - E[\Theta,\Phi], \tag{1}$$

$$R[\Theta,\Phi] = \frac{\alpha\mathcal{M}}{2\gamma}\int (\dot{\Theta}^2 + \sin^2\Theta\dot{\Phi}^2)\, dz, \tag{2}$$

where $\mathcal{M}$ is the magnetization per unit length, $E = \int \varepsilon\, dz$ is the total energy, γ is the absolute value of the gyromagnetic ratio, and α is the Gilbert damping parameter. Note that by calculating the Euler-Lagrange equations with respect to Θ and Φ one obtains the Landau-Lifshitz-Gilbert (LLG) equation in spherical coordinates [35]. Instead of dealing with (Θ,Φ) as continuously varying functions, we simplify the problem by making the ansatz $\Theta(z,t) = \Theta[z - Z(t)]$ and $\Phi(z,t) = \Psi(t)$, i.e., we assume rigid body motion and a spatially homogeneous polar angle. This way we introduce two collective coordinates, the position Z and the global tilt angle Ψ of the DW. Calculating the Euler-Lagrange equations for Z and Ψ with the boundary conditions $\lim_{z\to-\infty}\Theta = 0$ and $\lim_{z\to\infty}\Theta = \pi$ (which describes a head-to-head DW) yields the following coupled SDEs:

$$\begin{pmatrix} F_\Psi \\ F_Z \end{pmatrix} = \begin{pmatrix} \alpha\Gamma_\Psi & -2\mathcal{M}/\gamma \\ 2\mathcal{M}/\gamma & \alpha\Gamma_Z \end{pmatrix}\begin{pmatrix} \dot{\Psi} \\ \dot{Z} \end{pmatrix}, \tag{3}$$

where we introduce the abbreviations $\Gamma_\Psi = \mathcal{M}/\gamma\int\sin^2\Theta\ dz$ and $\Gamma_Z = \mathcal{M}/\gamma\int(\partial\Theta/\partial z)^2\ dz$. Note that for a tail-to-tail DW, the sign of the off-diagonal elements of the matrix on the right-hand side (r.h.s.) of Eq. (3) switches. This, however, leaves the MSDs in Z and Ψ unchanged and thus we restrict the following discussion to head-to-head DWs. Furthermore, it is important to note that inertia terms that would depend on $\ddot{\Psi}$ or $\ddot{Z}$ are absent in Eq. (3).

The forces F_λ, with $\lambda \in \{\Psi, Z\}$, in Eq. (3) can be separated into a deterministic part $F_\lambda^{\mathrm{det}} = -\partial E/\partial\lambda$ and a stochastic part F_λ^{th}, where the latter results from thermal fluctuations. For our study of Brownian motion we assume translational symmetry of the energy and consequently $F_Z^{\mathrm{det}} = 0$. The deterministic force acting on the DW angle F_Ψ^{det} depends on the details of the energy density ε. This is discussed in detail in Secs. II B and II C for uniaxial and biaxial systems, respectively.

Following Refs. [27,36], the stochastic forces are calculated via $F_\lambda^{\mathrm{th}} = -\mathcal{M}\partial/\partial\lambda[\int \boldsymbol{S}\cdot\boldsymbol{h}^{\mathrm{th}}\ dz]$, where $\boldsymbol{h}^{\mathrm{th}}$ describes the stochastic field within the continuum model with $\langle\boldsymbol{h}^{\mathrm{th}}(z,t)\rangle = 0$ and $\langle\boldsymbol{h}^{\mathrm{th}}(z,t)(\boldsymbol{h}^{\mathrm{th}})^{\mathrm{T}}(z',t')\rangle = 2k_{\mathrm{B}}T\alpha\mathbb{1}\delta(z-z')\delta(t-t')/(\gamma\mathcal{M})$. Within the rigid body approximation, it follows immediately that $\langle F_\lambda^{\mathrm{th}}\rangle = 0$ and the force autocorrelations is obtained as

$$\left\langle F_\lambda^{\mathrm{th}}(t)F_\lambda^{\mathrm{th}}(t')\right\rangle = 2\alpha k_{\mathrm{B}}T\Gamma_\lambda\delta(t-t'). \tag{4}$$

Note that the cross-correlation term vanishes, i.e., $\langle F_Z^{\mathrm{th}}(t)F_\Psi^{\mathrm{th}}(t')\rangle = 0$. Inserting these stochastic forces into Eq. (3) yields a set of coupled Langevin-type equations of motion for the DW position and angle. Both the fluctuations as well the dissipation in these equations depend on $\alpha\Gamma_\lambda$, in agreement with the fluctuation-dissipation theorem [37].

B. Brownian motion in uniaxial systems

For a uniaxial system the energy of the spin configuration is independent of Ψ and, as a consequence, the deterministic force acting on the DW angle F_Ψ^{det} vanishes. Henceforth, Eq. (3) becomes a two-dimensional first order linear SDE, which can be solved exactly using stochastic calculus. Without loss of generality we assume the initial condition $\lambda(0) = 0$, with $\lambda \in \{\Psi, Z\}$ as above.

The velocities $\dot{\lambda}$ can be expressed in terms of the stochastic forces by inverting the matrix on the r.h.s. of Eq. (3). It immediately follows that $\langle\Delta\lambda(t)\rangle = \langle\lambda(t) - \lambda(0)\rangle = \langle\lambda(t)\rangle \equiv 0$, as expected for Brownian motion, due to vanishing mean values of the stochastic forces.

In order to calculate the MSDs from Eq. (4), we first calculate the velocity autocorrelations $\langle\dot{\lambda}(t')\dot{\lambda}(t'')\rangle$, where the force autocorrelation (4) is used. Performing two time integrations $\int_0^t(\cdots)\ dt'$ and $\int_0^t(\cdots)\ dt''$ of the velocity autocorrelations yield the MSDs as $\langle\Delta\Psi^2(t)\rangle = 2D_\Psi^{\mathrm{uni}}t$, $\langle\Delta Z^2(t)\rangle = 2D_Z^{\mathrm{uni}}t$, and $\langle\Delta\Psi(t)\Delta Z(t)\rangle = 0$ with the diffusion coefficients

$$D_\Psi^{\mathrm{uni}} = k_{\mathrm{B}}T\frac{\alpha\Gamma_Z}{\alpha^2\Gamma_\Psi\Gamma_Z + (2\mathcal{M}/\gamma)^2}, \tag{5}$$

$$D_Z^{\mathrm{uni}} = k_B T \frac{\alpha \Gamma_\Psi}{\alpha^2 \Gamma_\Psi \Gamma_Z + (2\mathcal{M}/\gamma)^2}. \tag{6}$$

The above expressions predict a peculiar dependence of the Brownian motion on the Gilbert damping α. Usually, the diffusion coefficient of a particle is enhanced if the friction is lowered. For DWs in uniaxial nanowires the situation is drastically different: the diffusion coefficients show a gradual drop to zero with decreasing α. This observation has its origin in the off-diagonal elements in Eq. (3) and is very similar to what was reported for the Brownian motion of skyrmions [38]. This similarity follows from the fact that Eq. (3) in the absence of external forces is analogous to the stochastic Thiele equation for the description of Brownian motion of skyrmions [27,36,38–40]. As such, Eq. (3) describes Brownian gyromotion [41] of the DW in Ψ and Z. We also want to emphasize the fact that our analytical calculations predict that the MSDs of DWs in uniaxial systems do not show inertia effects, i.e., they are linear in t at all times.

C. Brownian motion in biaxial systems

When the rotational symmetry with respect to the easy axis is broken, the energy of the spin configuration depends on the DW angle Ψ. A simple example for a system with broken rotational symmetry is a biaxial nanowire. There, the presence of an intermediate axis gives rise to an angular potential that can be written as $E(\Psi) = -\Delta E \cos(2\Psi)/2$, with ΔE being the height of the energy barrier preventing a flip of the magnetization of the domain wall (see Sec. II D for details). The deterministic force induced by this potential is calculated as $F_\Psi^{\mathrm{det}} = \Delta E \sin(2\Psi)$. Consequently, Eq. (3) is a nonlinear SDE and an exact calculation of the MSDs is impossible.

Hence, we restrict the following calculations to the case $k_B T \ll \Delta E$, i.e., the energy barrier is much larger than the thermal energy. In this regime, $E(\Psi)$ can be well approximated by a Taylor expansion up to second order. This way, an exact solution of Eq. (3) is possible and the approximation is often justified, since ΔE scales with the number of spins within the DW. It fails, however, for high temperatures, small anisotropy constants along the intermediate axis, or narrow DWs in thin wires. This regime is studied in this work within atomistic spin dynamics simulations, which reveal the emergence of a diffusive Walker breakdown that is discussed in detail in Sec. III C.

Expanding $E(\Psi)$ up to second order in Ψ around Ψ_{eq} and inserting into Eq. (3) yields

$$\begin{pmatrix} F_\Psi^{\mathrm{th}} \\ F_Z^{\mathrm{th}} \end{pmatrix} = \begin{pmatrix} \alpha\Gamma_\Psi & -2\mathcal{M}/\gamma \\ 2\mathcal{M}/\gamma & \alpha\Gamma_Z \end{pmatrix} \begin{pmatrix} \dot{\Psi} \\ \dot{Z} \end{pmatrix} + \begin{pmatrix} \kappa & 0 \\ 0 & 0 \end{pmatrix} \begin{pmatrix} \Psi \\ Z \end{pmatrix}, \tag{7}$$

where we introduced the spring constant $\kappa = \partial^2 E/\partial \Psi^2|_{\Psi_{\mathrm{eq}}}$. Without loss of generality we assume $\Psi_{\mathrm{eq}} = 0$. Note that the approximative description of DWs via Eq. (7) is not only valid for biaxial systems, but for any system with broken rotational symmetry (e.g., due to the presence of DMI or a perpendicular magnetic field, see Appendix B).

Equation (7) describes an Ornstein-Uhlenbeck stochastic process for which the solution can be found in literature (e.g., in Ref. [42]). The time evolution of the mean values of DW position and angle as well as the MSDs can be calculated from this solution. A detailed discussion of this calculation can be found in Appendix A. We obtain

$$\langle \Delta\Psi(t) \rangle = \left(e^{-\kappa \beta D_\Psi^{\mathrm{uni}} t} - 1 \right) \langle \Psi(0) \rangle , \tag{8}$$

$$\langle \Delta Z(t) \rangle = -\frac{2\mathcal{M}/\gamma}{\alpha \Gamma_Z} \left(e^{-\kappa \beta D_\Psi^{\mathrm{uni}} t} - 1 \right) \langle \Psi(0) \rangle , \tag{9}$$

where we introduced $\beta = 1/(k_B T)$. Equation (8) describes a relaxation of Ψ to its equilibrium value, which, due to the coupling between $\dot{\Psi}$ and $\dot{Z}$ via the off-diagonal elements in Eq. (7), gives rise to the time dependence in Eq. (9). In the following, however, we assume that $\langle \Psi(0) \rangle = 0$, which leads to vanishing mean values for $\langle \Delta\Psi(t) \rangle$ and $\langle \Delta Z(t) \rangle$ at all times.

For the MSDs we then obtain (see Appendix A)

$$\langle \Delta\Psi^2(t) \rangle = \frac{k_B T}{\kappa} \left(1 - e^{-2\kappa \beta D_\Psi^{\mathrm{uni}} t} \right), \tag{10}$$

$$\langle \Delta Z^2(t) \rangle = 2 \frac{k_B T}{\alpha \Gamma_z} \left\{ t + \frac{(2\mathcal{M}/\gamma)^2}{2\alpha \Gamma_Z \kappa} \times \left[1 - \left(2 - e^{-\kappa \beta D_\Psi^{\mathrm{uni}} t} \right)^2 \right] \right\}. \tag{11}$$

In the limit $\kappa \to 0$, the above expressions reduce to those obtained for the uniaxial case, with the diffusion coefficients as given by Eqs. (5) and (6).

The nontrivial time dependence in Eqs. (10) and (11) can be understood by introducing a transition time $t^{\mathrm{trans}} = k_B T/(D_\Psi^{\mathrm{uni}} \kappa)$ with distinct behavior for $t \ll t^{\mathrm{trans}}$ or $t \gg t^{\mathrm{trans}}$:

$$\langle \Delta\Psi^2(t) \rangle = \begin{cases} 2D_\Psi^{\mathrm{uni}} t, & \text{for } t \ll t^{\mathrm{trans}}, \\ k_B T/\kappa, & \text{for } t \gg t^{\mathrm{trans}}, \end{cases} \tag{12}$$

$$\langle \Delta Z^2(t) \rangle = \begin{cases} 2D_Z^{\mathrm{uni}} t, & \text{for } t \ll t^{\mathrm{trans}}, \\ 2D_Z^{\mathrm{bi,harm}} t, & \text{for } t \gg t^{\mathrm{trans}}. \end{cases} \tag{13}$$

In the short term limit, the diffusive motion is the same as in the uniaxial case. This is because the angle does not experience the impact of the potential as long as it is in the vicinity of the equilibrium value. Hence, the DW moves as if the potential was absent. In the long term limit, $\langle \Delta\Psi^2(t) \rangle$ converges to its equilibrium value $k_B T/\kappa$. This result can be calculated straightforwardly via the equipartition theorem: since we treat the potential in harmonic approximation, it follows that $\langle E \rangle_{\mathrm{eq}} = \kappa \langle \Delta\Psi^2 \rangle_{\mathrm{eq}}/2 = k_B T/2$. Once the angular MSD is converged, the exponential function in Eq. (11) vanishes. $\langle \Delta Z^2(t) \rangle$ then grows linearly with t and we can identify the diffusion coefficient for DWs in a biaxial system in harmonic approximation of the angular potential as

$$D_Z^{\mathrm{bi,harm}} = \frac{k_B T}{\alpha \Gamma_z}. \tag{14}$$

Equation (14) reproduces the usual dependence on friction: diffusive motion is enhanced when friction is lowered. Note though that this is in contrast to uniaxial systems, see Eq. (6). Thus, for typical values of the Gilbert damping (10^{-1} to 10^{-4}) we expect that Brownian motion of DWs in systems with broken rotational symmetry is at least 2 orders of magnitude higher than for uniaxial systems.

Note that Eq. (14) was already derived in an earlier work [27], where the authors neglected the dynamics of the DW angle. In that case, the effective equation of motion for ferromagnetic DWs, Eq. (3), reduces to the overdamped Langevin equation $\alpha\Gamma_Z\dot{Z} = F_Z^{\text{th}}$, from which Eq. (14) follows directly. However, in that approximative single-variable approach, the complex time dependence of MSDs in the inertial regime is missing. In addition, that approach is not suited for the description of the dynamics of uniaxial DWs. We also want to point out that the results of a single-variable approach including a Döring-mass term [15,43], which was discussed in Ref. [27] as well, also differs from the two-variable description of the DW dynamics established here. This is examined in detail in Appendix C.

We again want to emphasize that the calculations in this subsection are only valid as long as the fluctuations of the DW angle are small. However, if k_BT is comparable to ΔE, the harmonic approximation of the angular potential breaks down, giving rise to a Walker breakdown of DW Brownian motion (see Sec. III C).

D. Prototypical uni- and biaxial systems

So far our results were independent of the specific energy density ε in the Lagrangian (1), apart from the fact that an easy axis along the nanowire was assumed. Hereinafter we derive analytical expressions for Γ_Ψ, Γ_Z, κ, and the diffusion coefficients based on the standard energy density for the description of one-dimensional uni- and biaxial ferromagnets [15],

$$\varepsilon(\Theta,\Phi) = A\left[\left(\frac{\partial\Theta}{\partial z}\right)^2 + \sin^2\Theta\left(\frac{\partial\Phi}{\partial z}\right)^2\right] - K_z\cos^2\Theta - K_x\cos^2\Phi\sin^2\Theta, \tag{15}$$

with the exchange constant A, the anisotropies along the easy axis K_z, and along the intermediate axis K_x with $K_z > K_x \geqslant 0$.

The above energy density is minimized by the usual ansatz for a head-to-head DW with $\Phi(z) = \Psi$ and $\Theta(z) = \arccos[-\tanh(z/\Delta)]$, where Δ is the DW width [15]. Inserting this ansatz into Eq. (15) and spatial integration yields the energy of a domain wall as

$$E(\Psi,\Delta) = 2\frac{A}{\Delta} + 2\Delta(K_z - K_x\cos^2\Psi) + E_0, \tag{16}$$

where E_0 is the irrelevant energy of the homogeneous state. The above expression is minimized by $\Psi/\pi \in \mathbb{Z}$ and $\Delta = \sqrt{A/(K_z - K_x)}$. Harmonic expansion around this minimum yields for the spring constant $\kappa = 4\Delta K_x$. In addition, it follows from Eq. (16) that the angular energy barrier for a biaxial system introduced in Sec. II C is given by

$$\Delta E = 2\Delta K_x. \tag{17}$$

This DW profile can be used to evaluate the expressions derived in Secs. II B and II C. The diagonal parameters of the matrix on the r.h.s. of Eq. (3) are then

$$\Gamma_\Psi = \frac{2\mathcal{M}}{\gamma}\Delta \quad \text{and} \quad \Gamma_Z = \frac{2\mathcal{M}}{\gamma}\frac{1}{\Delta}. \tag{18}$$

Inserting these expressions into Eqs. (5) and (6) for the uniaxial diffusion coefficient and into Eq. (14) for the biaxial diffusion coefficient in harmonic approximation yields

$$D_\lambda^{\text{uni}} = k_BT\frac{\gamma}{2\mathcal{M}}\frac{\alpha}{1+\alpha^2}\begin{cases}\frac{1}{\Delta}, & \text{for } \lambda = \Psi,\\ \Delta, & \text{for } \lambda = Z,\end{cases} \tag{19}$$

$$D_Z^{\text{bi,harm}} = k_BT\frac{\gamma}{2\mathcal{M}}\Delta\frac{1}{\alpha}. \tag{20}$$

Apart from temperature and Gilbert damping, the diffusion coefficients depend only on the DW width. While the diffusion coefficient for Z is proportional to the width of the DW, that of Ψ is inversely proportional to it. For uniaxial systems the ratio between both coefficients is given by $\Delta^2 = A/K_z$ with typically $A \gg K_z$. Hence, very broad DWs will show strong Brownian motion in the position Z but only small Brownian motion in the angle Ψ. The transition time for biaxial systems in harmonic approximation follows as

$$t^{\text{trans}} = \frac{2\mathcal{M}}{\gamma}\frac{1+\alpha^2}{\alpha}\frac{1}{4K_x} \tag{21}$$

and is found to be independent of the DW width.

The calculations presented here can be straightforwardly generalized to systems with additional contributions to the energy density given by Eq. (15). This is done for DMI and perpendicular magnetic fields in Appendix B.

III. ATOMISTIC SPIN DYNAMICS SIMULATIONS

For our numerical study we simulate the Brownian motion of a DW based on a model of normalized classical spins $\boldsymbol{S}_i = \boldsymbol{\mu}_i/\mu_s$ located on a simple cubic lattice, with μ_s being the atomic magnetic moment. We consider isotropic Heisenberg exchange interactions for nearest neighbors and a uni- or biaxial anisotropy. The Hamiltonian reads

$$\mathcal{H} = -\frac{J}{2}\sum_{i,j}\boldsymbol{S}_i\cdot\boldsymbol{S}_j - d_z\sum_i\left(S_i^z\right)^2 - d_x\sum_i\left(S_i^x\right)^2, \tag{22}$$

with $J > 0$ for ferromagnetic order and $d_z > d_x \geqslant 0$. We use $J = 10\,\text{meV}$ and $d_z = 1\,\text{meV}$. When describing a uniaxial system, the anisotropy along the intermediate axis is $d_x = 0$. Biaxial systems are characterized by a finite d_x and we use a value of $d_x = 0.1\,\text{meV}$ to simulate a system with large angular energy barrier and $d_x = 0.01\,\text{meV}$ for a system with small angular energy barrier as compared to thermal fluctuations.

The dynamics of the spins is calculated using the stochastic LLG equation [35]

$$(1+\alpha^2)\frac{\partial\boldsymbol{S}_i}{\partial t} = -\frac{\gamma}{\mu_s}\boldsymbol{S}_i\times\left(\boldsymbol{H}_i^{\text{eff}} + \alpha\boldsymbol{S}_i\times\boldsymbol{H}_i^{\text{eff}}\right), \tag{23}$$

with the effective field $\boldsymbol{H}_i^{\text{eff}} = -\partial\mathcal{H}/\partial\boldsymbol{S}_i + \boldsymbol{\zeta}_i$ containing both the deterministic contribution from the Hamiltonian (22) as well as a stochastic field $\boldsymbol{\zeta}_i$ with the properties $\langle\boldsymbol{\zeta}_i\rangle = 0$ and

$$\left\langle\boldsymbol{\zeta}_i(t)\boldsymbol{\zeta}_j^{\text{T}}(t')\right\rangle = \frac{2\alpha\mu_sk_BT}{\gamma}\delta_{ij}\delta(t-t'). \tag{24}$$

For our simulations we use $\mu_s = 2\mu_{\text{Bohr}}$ and $\gamma = 1.76\times10^{11}\,\text{s}^{-1}\,\text{T}^{-1}$. We simulate an elongated system with 128 spins along the z axis and a cross section of 16×16 spins for the uniaxial system and the biaxial system with large angular

energy barrier and a cross section of 6×6 spins for the biaxial system with a small angular energy barrier. Unless stated otherwise, the temperature has a fixed value of $k_B T = 0.1\,\text{meV}$. Furthermore, we apply periodic boundary conditions along x and y axis and open boundary conditions along z axis.

The simulations are performed via a GPU-accelerated implementation of Heun's method [35] with a fixed time step of 0.1 fs. Initially, a tail-to-tail DW is placed in the center of the system and thermalized at finite temperature. Subsequently, its position and angle are calculated from the spin configuration every 0.1 ps over 1.5 ns via

$$Z(t) = \frac{\sum_i \rho(\boldsymbol{S}_i) z_i}{\sum_i \rho(\boldsymbol{S}_i)}, \tag{25}$$

$$\Psi(t) = \frac{\sum_i \rho(\boldsymbol{S}_i) \arctan\left(S_i^y / S_i^x\right)}{\sum_i \rho(\boldsymbol{S}_i)}, \tag{26}$$

with $\rho(\boldsymbol{S}_i) = 1 - (S_i^z)^2$, yielding the trajectory of a DW. The MSDs are obtained by averaging over multiple trajectories via $\langle \Delta Z^2(t) \rangle = 1/N \sum_{n=1}^{N} \Delta Z_n^2(t)$ and $\langle \Delta \Psi^2(t) \rangle = 1/N \sum_{n=1}^{N} \Delta \Psi_n^2(t)$, with N being the number of trajectories. The diffusion coefficients are obtained by performing linear fits to the MSDs in the interval between 0.5 ns (to eliminate nonlinear inertia effects) and 1.5 ns (simulation time). Within this interval, DWs exhibit normal diffusion for all parameters sets used in this work.

For the conversion between atomistic and continuum approach parameters introduced in Sec. II D, the following relations apply: $A = J t_x t_y/(2a)$, $K_z = d_z t_x t_y / a^3$, $K_x = d_x t_x t_y / a^3$, and $\mathcal{M} = \mu_s t_x t_y / a^3$, where a is the lattice constant and t_x, t_y are the dimensions in the cross section.

A. Uniaxial systems

The results of the simulations of a uniaxial system and the corresponding analytical predictions obtained within the collective coordinate approach are compared in Fig. 1. We find very good agreement for a wide range of values for the Gilbert damping parameter. The results also confirm a ratio of $\Delta^2 \approx 5a^2$ between the Brownian motion of the DW position and the DW angle. Figure 1(a) shows the MSDs of DW position and angle. At the timescale of this figure, no nonlinear behavior is visible, demonstrating the absence of inertia for the motion of DWs in uniaxial ferromagnets. Figure 1(b) shows the diffusion coefficients versus Gilbert damping parameter. Our numerical results verify the theoretically predicted peculiar dependence of the diffusion coefficients in uniaxial systems on damping: with decreasing dissipation, the diffusive motion is lowered. This is analogous to what was demonstrated in simulations of the diffusion of skyrmions [27,36], and has its origin in the presence of the antisymmetric off-diagonal components of the matrix on the r.h.s. of Eq. (3).

B. Biaxial systems with large angular potential

In this subsection we compare the numerical results for the Brownian motion of a DW in a biaxial system with a large angular potential with the theoretical predictions obtained in harmonic approximation of this potential (for details see Sec. II C). For the simulation parameters used here (cf. Sec. III), the angular energy barrier can be estimated as $\Delta E \approx$ 120 meV using Eq. (17), which is three orders of magnitude larger than the thermal energy (and nearly one order of magnitude larger than the Curie temperature).

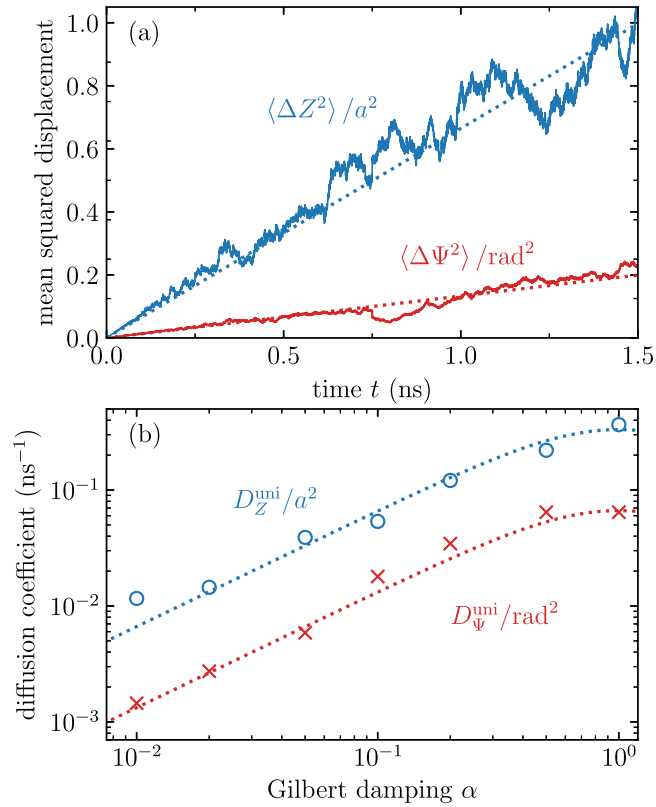

FIG. 1. Simulation results (solid lines and symbols) and theoretical predictions (dotted lines) based on Eq. (19) for Brownian motion of a uniaxial DW. (a) Mean squared displacements $\langle \Delta \Psi^2(t) \rangle$ and $\langle \Delta Z^2(t) \rangle / a^2$ for $\alpha = 1.0$. (b) Diffusion coefficients versus Gilbert damping parameter α.

The validity of the harmonic approximation of the angular potential is demonstrated in Fig. 2. Again we find perfect agreement between our numerical results and the analytical predictions. Figures 2(a) and 2(b) show the MSDs of DW position and angle and clearly demonstrate the emergence of a transition from the short term quasi-uniaxial to the long term regime, where the angular MSD is converged to $\langle \Psi \rangle_{\text{eq}} = k_B T / \kappa$, as predicted by the equipartition theorem. In addition, we want to emphasize the drastically enhanced diffusion in Z as compared to the uniaxial case, due to the inverse proportionality to α. As demonstrated in Fig. 2(c), the diffusion coefficient of a biaxial DW is orders of magnitude larger than that of a uniaxial one for typical values of the Gilbert damping parameter.

C. Walker breakdown of Brownian motion

For our simulations of the diffusive Walker breakdown, we use a value of $d_x = 0.01\,\text{meV}$ and a cross section of 6×6 spins, yielding an energy barrier of $\Delta E \approx 1.62\,\text{meV}$ based on Eq. (17). In terms of thermal energy, this energy barrier can be used to define a temperature, hereinafter referred to as Walker temperature, via $T^{\text{Walker}} = \Delta E / k_B$.

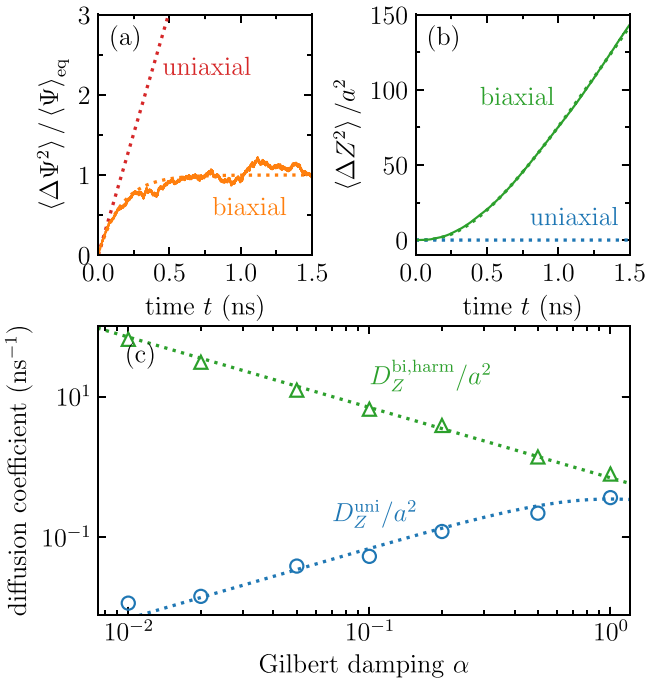

FIG. 2. Simulation results (solid lines and symbols) for Brownian motion of DWs in biaxial systems with large angular potential in comparison with theoretical predictions (dotted lines as labeled). (a) and (b) Mean squared displacements $\langle \Delta\Psi^2(t) \rangle$ normalized to the equilibrium value $\langle \Delta\Psi^2 \rangle_{eq} = k_B T/\kappa$ and $\langle \Delta Z^2(t) \rangle / a^2$ for $\alpha = 0.01$. The dotted lines are Eqs. (10) and (11) evaluated using the results from Sec. II D. (c) Diffusion coefficient of DWs in uniaxial systems and biaxial systems with large angular potential versus α in comparison with analytical predictions based on Eqs. (19) (blue) and (20) (green).

Figure 3 shows the diffusion coefficients of the DW position for temperatures ranging from 0 to approximately $2T^{\text{Walker}}$ and for $\alpha = 0.1$. Initially, the simulation results increase linearly with temperature following our prediction for the diffusion coefficient obtained in harmonic approximation of the angular potential $D_Z^{\text{bi,harm}}$. At intermediate temperatures, however, the behavior changes completely. Surprisingly, we find a maximum for the diffusion coefficient at roughly one third of T^{Walker} with a subsequent decay for increasing temperature. Finally, the diffusion coefficient appears to converge towards the value for a uniaxial system D_Z^{uni}.

Qualitatively, this observation can be understood as follows. As long as the thermal energy is small compared to ΔE, the DW angle is restricted to values close to equilibrium and the harmonic approximation for the potential is valid. Thus, the diffusion coefficient of the DW position is inversely proportional to the Gilbert damping parameter (see Sec. III B), giving rise to the steep initial slope in Fig. 3. If the thermal energy is very large in comparison with the angular potential, the DW angle can easily overcome the energy barrier. Hence, the impact of the angular potential can be neglected and the DW is expected to exhibit quasi-uniaxial behavior. In the uniaxial case, the diffusion coefficient is proportional to $\alpha/(1+\alpha^2)$ (see Sec. III A) and therefore drastically reduced (here it is roughly two orders of magnitude lower, since $\alpha = 0.1$).

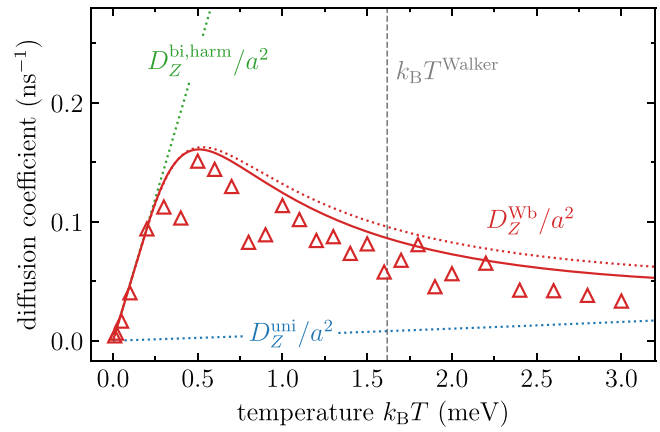

FIG. 3. Walker breakdown of Brownian DW motion. Simulation results (symbols) for diffusion coefficients of the DW position are compared with theoretical predictions based on Eqs. (19) (blue) and (20) (green) and (27) using constant (red dotted line) and temperature-dependent parameters (red solid line) for $\alpha = 0.1$. The gray dashed line marks the Walker temperature $k_B T^{\text{Walker}} = \Delta E$.

Therefore, although the higher temperature would normally lead to an enhancement of the diffusion coefficient, this is overcompensated by a transition from a regime where the dynamics are dominated by the angular potential to a regime with quasi-uniaxial behavior. Note that we expect this effect to be even more pronounced for smaller values of the Gilbert damping parameter. In analogy to what is well established for the dynamics of DWs driven by external fields, currents, or temperature gradients [13,17,18], this phenomena can be interpreted as the Walker breakdown of Brownian DW motion. In contrast to the Walker breakdown induced by deterministic driving forces, this Walker breakdown is not a sharp transition, due to the finite probability of overcoming the angular energy barrier, even at temperatures way below T^{Walker}.

Even though an exact calculation of the diffusive Walker breakdown via Eq. (3) for the full cosine potential is impossible (cf. Sec. II C), a quantitative approximation can be obtained by the following ad-hoc approach. As argued above, for low and high temperatures the DW diffusion coefficients follow $D_Z^{\text{bi,harm}}$ and D_Z^{uni}, respectively. We make the following ansatz for the transition between these two regimes:

$$D_Z^{\text{Wb}} = \eta[\beta E(\Psi)] D_Z^{\text{uni}} + \{1 - \eta[\beta E(\Psi)]\} D_Z^{\text{bi,harm}}, \tag{27}$$

$$D_\Psi^{\text{Wb}} = \eta[\beta E(\Psi)] D_\Psi^{\text{uni}}, \tag{28}$$

where $\eta[\beta E(\Psi)] \in [0, 1]$ is a yet-to-be-determined weighting factor that depends on temperature and on the angular potential. Note that for very low/high temperatures, $\eta[\beta E(\Psi)]$ must go to zero/one, in order to describe the observed transition. As such, Eq. (28) can be interpreted as the reduction of the effective diffusion coefficient in the presence of a periodic potential [44]. To a first approximation we estimate $\eta[\beta E(\Psi)]$ using the Lifson-Jackson formula $\eta[\beta E(\Psi)] = (\langle e^{\beta E(\Psi)} \rangle \langle e^{-\beta E(\Psi)} \rangle)^{-1}$, where $\langle \cdots \rangle$ is the average over one period of the potential [45]. In a biaxial system, the angular potential has a cosine form, $E(\Psi) = -\Delta E \cos(2\Psi)/2$, for which the Lifson-

Jackson formula yields $\eta[\beta E(\Psi)] = [I_0(\beta\Delta E/2)]^{-2}$, with $I_n(x)$ being the modified Bessel function of the first kind.

Inserting this expression into Eq. (27), we obtain a formula describing the diffusive Walker breakdown that is represented by the red dotted line in Fig. 3. Even better quantitative agreement can be achieved by assuming temperature-dependent exchange parameters (red solid line). For that, following Refs. [46,47], we assume $A(T) \sim m(T)^2$ and $K_{x/z}(T) \sim m(T)^3$, with $m(T)$ being the temperature-dependent magnetization. By comparison with simulation data, we find that $m(T) \approx [1.0 - k_B T/(1.44J)]^{0.32}$. Using the temperature-dependent exchange parameters introduced above, together with the formulas in Sec. II D, the scaling of the diffusion coefficients of the DW position and the angular potential barrier with temperature can be estimated as

$$D_Z^{\mathrm{uni/bi,harm}}(T) \sim m(T)^{-3/2}, \tag{29}$$

$$\Delta E(T) \sim m(T)^{5/2}, \tag{30}$$

indicating that both effects are competing: while the former leads to higher Brownian motion, since the magnetization goes down with increasing temperature, the latter leads to lower Brownian motion, because the angular energy barrier becomes lower, which facilitates the transition to the quasi-uniaxial regime. As demonstrated in Fig. 3, we find that the reduction of the angular energy barrier is the dominating factor of including temperature-dependent exchange parameters. The resulting curve (red solid line) agrees well with the simulation results, although it still slightly overestimates the diffusion coefficients, especially at high temperatures.

IV. CONCLUSION

We studied the Brownian motion of DWs in uni- and biaxial nanowires using analytical calculations based on a collective coordinate approach and large-scale atomistic spin dynamics simulations based on the stochastic LLG equation.

We revealed that both the position and the angle of a DW in uniaxial ferromagnets show Brownian motion and that the ratio between the respective diffusion coefficients is given by the squared DW width. These diffusion coefficients were found to exhibit a peculiar dependence on damping: Brownian motion is reduced for low damping. This behavior is very similar to what was observed for skyrmions and has its origin in the antisymmetric off-diagonal components in the effective equation of motion. In addition, we found that the Brownian motion of uniaxial DWs is inertia free, i.e., the MSDs scale linearly with time for all times. This is due the absence of a mass term in the effective equation of motion.

The situation in biaxial systems is more complex. As long as thermal energy is small compared to the angular potential, the translational Brownian motion is greatly enhanced as compared to the uniaxial case and the corresponding diffusion coefficient was found to be inversely proportional to damping. This is in quantitative agreement with our theoretical predictions obtained in a harmonic approximation of the angular potential. If thermal energies are comparable to the angular potential, we found a peculiar behavior of the diffusion coefficient of the DW position: at low temperatures, the diffusion coefficient scales linearly with temperature, following the prediction for large angular potentials, up to a certain threshold temperature, where the chance that the DW overcomes the angular potential barrier due to thermal fluctuations becomes relevant. In the vicinity of this threshold, the diffusion coefficient has a maximum, followed by a subsequent decrease upon further increase of temperature. This can be understood by the fact that for very large temperatures the angular potential becomes irrelevant and the DW shows quasi-uniaxial dynamics, with a greatly reduced diffusion coefficient. We termed this behavior *Walker breakdown of Brownian motion*, in analogy to the Walker breakdown of deterministic motion [13].

The threshold temperature for this type of Walker breakdown depends on the leading term that breaks the rotational symmetry as well as the activation volume. As such, it is highly material and geometry specific and can vary between, e.g., more than 10^5K for a permalloy nanowire with fairly relevant cubic anisotropy [48] to values that are certainly below the critical temperature for permalloy on GaAs(001) with vanishingly small anisotropy at an iron concentration of about 25% [49].

The emergence of a diffusive Walker breakdown also opens up a new pathway for the efficient control of DW diffusion. Based on the fact that the diffusion coefficient crucially depends on the ratio between thermal energy and the angular potential and that the latter can be induced by a perpendicular magnetic field (see Appendix B), we propose that varying the perpendicular field can change the diffusion coefficient of DWs by orders magnitude at fixed temperatures.

ACKNOWLEDGMENT

This work was financially supported by the Deutsche Forschungsgemeinschaft via Project No. 403502522 and the SFB 1432.

APPENDIX A: DERIVATION OF MEAN SQUARED DISPLACEMENTS IN BIAXIAL SYSTEMS IN HARMONIC APPROXIMATION

The dynamics of DWs in biaxial ferromagnets can be described in terms of a collective coordinate approach. In harmonic approximation we obtain (see Sec. II C)

$$\begin{pmatrix} F_\Psi^{\mathrm{th}} \\ F_Z^{\mathrm{th}} \end{pmatrix} = \begin{pmatrix} \alpha\Gamma_\Psi & -2\mathcal{M}/\gamma \\ 2\mathcal{M}/\gamma & \alpha\Gamma_Z \end{pmatrix} \begin{pmatrix} \dot{\Psi} \\ \dot{Z} \end{pmatrix} + \begin{pmatrix} \kappa & 0 \\ 0 & 0 \end{pmatrix} \begin{pmatrix} \Psi \\ Z \end{pmatrix}, \tag{A1}$$

where the force correlation with $\lambda \in \{\Psi, Z\}$ is given by

$$\left\langle F_\lambda^{\mathrm{th}}(t) F_\lambda^{\mathrm{th}}(t') \right\rangle = 2\alpha k_B T \Gamma_\lambda \delta(t - t'). \tag{A2}$$

Equation (A1) is a first order linear SDE equation that describes a two-dimensional Ornstein-Uhlenbeck process [42]. Equivalently, it can be rewritten as

$$d\boldsymbol{x}_t = -\Omega \boldsymbol{x}_t dt + \sigma d\boldsymbol{W}_t, \tag{A3}$$

where $\boldsymbol{x}_t = (\Psi(t), Z(t))^{\mathrm{T}}$ and $\boldsymbol{W}_t$ denotes the Wiener process [50]. Ω and σ are 2×2 matrices that can be obtained by comparison with Eq. (A1) and read

$$\Omega = \frac{\kappa}{\alpha^2 \Gamma_\Psi \Gamma_Z + (2\mathcal{M}/\gamma)^2} \begin{pmatrix} \alpha\Gamma_Z & 0 \\ -2\mathcal{M}/\gamma & 0 \end{pmatrix}, \tag{A4}$$

$$\sigma=\frac{\sqrt{2\alpha k_\mathrm{B}T}}{\alpha^2\Gamma_\Psi\Gamma_Z+(2\mathcal{M}/\gamma)^2}\begin{pmatrix}\alpha\Gamma_Z\sqrt{\Gamma_\Psi} & (2\mathcal{M}/\gamma)\sqrt{\Gamma_Z}\\ -2\mathcal{M}/\gamma\sqrt{\Gamma_\Psi} & \alpha\Gamma_\Psi\sqrt{\Gamma_Z}\end{pmatrix}. \tag{A5}$$

Following Ref. [42], the solution of Eq. (A3) is given by

$$\boldsymbol{x}_t = e^{-\Omega t}\boldsymbol{x}_0 + \int_0^t e^{-\Omega(t-t')}\sigma\, d\boldsymbol{W}_{t'} \tag{A6}$$

and the mean of the above expression and the corresponding second moment matrix can be calculated as

$$\langle \boldsymbol{x}_t\rangle = e^{-\Omega t}\,\langle \boldsymbol{x}_0\rangle\,, \tag{A7}$$

$$\begin{aligned}\left\langle \boldsymbol{x}_t\boldsymbol{x}_t^\mathrm{T}\right\rangle &= e^{-\Omega t}\,\langle \boldsymbol{x}_0\rangle\,(e^{-\Omega t}\,\langle \boldsymbol{x}_0\rangle)^\mathrm{T}\\ &\quad+\left\langle \int_0^t e^{-\Omega(t-t')}\sigma\, d\boldsymbol{W}_{t'}\left(\int_0^t e^{-\Omega(t-t'')}\sigma\, d\boldsymbol{W}_{t''}\right)^\mathrm{T}\right\rangle.\end{aligned} \tag{A8}$$

Using the rules for matrix exponentials we obtain

$$e^{-\Omega t} = \begin{pmatrix} e^{-\kappa\beta D_\Psi^\mathrm{uni}t} & 0\\ \frac{2\mathcal{M}/\gamma}{\alpha\Gamma_Z}\left(1-e^{-\kappa\beta D_\Psi^\mathrm{uni}t}\right) & 1\end{pmatrix}. \tag{A9}$$

Inserting the above expression into Eqs. (A7) and (A8) and using stochastic calculus yields

$$\langle\Delta\Psi(t)\rangle = \left(e^{-\kappa\beta D_\Psi^\mathrm{uni}t}-1\right)\langle\Psi(0)\rangle\,, \tag{A10}$$

$$\langle\Delta Z(t)\rangle = -\frac{2\mathcal{M}/\gamma}{\alpha\Gamma_Z}\left(e^{-\kappa\beta D_\Psi^\mathrm{uni}t}-1\right)\langle\Psi(0)\rangle\,, \tag{A11}$$

$$\langle\Delta\Psi^2(t)\rangle = \langle\Delta\Psi(t)\rangle^2 + \frac{k_\mathrm{B}T}{\kappa}\left(1-e^{-2\kappa\beta D_\Psi^\mathrm{uni}t}\right), \tag{A12}$$

$$\begin{aligned}\langle\Delta Z^2(t)\rangle &= \langle\Delta Z(t)\rangle^2 + 2\frac{k_\mathrm{B}T}{\alpha\Gamma_z}\left\{t+\frac{(2\mathcal{M}/\gamma)^2}{2\alpha\Gamma_Z\kappa}\right.\\ &\quad\left.\times\left[1-\left(2-e^{-\kappa\beta D_\Psi^\mathrm{uni}t}\right)^2\right]\right\}.\end{aligned} \tag{A13}$$

If we assume that $\langle\Psi(0)\rangle = 0$, Eqs. (A12) and (A13) reduce to Eqs. (10) and (11), respectively.

APPENDIX B: ANGULAR POTENTIALS INDUCED BY PERPENDICULAR MAGNETIC FIELDS AND BY DMI

In Secs. III B and III C we have demonstrated for biaxial systems that the emergence of the drastically enhanced diffusion coefficient, as compared to uniaxial systems, and the diffusive Walker breakdown are linked to the presence of an angular potential. Such a potential can also be induced by other symmetry-breaking contributions to the energy. Although the explicit form of the respective angular potentials might differ from the one obtained for a biaxial system, we expect that the features found for the Brownian motion of DWs are very similar. We also want to emphasize that the analytical formulas for the MSDs and the diffusion coefficient derived in harmonic approximation of the angular potential in Sec. II C are valid for any potential and therefore also applicable to systems with perpendicular magnetic fields or DMI.

Hereinafter we derive analytical expressions for the domain wall width, the angular potential, and the spring constant for uniaxial systems with a perpendicular magnetic field and with DMI, respectively. In doing so, we again use the usual ansatz for a head-to-head DW (see Sec. II D) with

$$\begin{aligned}\Phi(z) &= \Psi,\\ \Theta(z) &= \arccos[-\tanh(z/\Delta)]\end{aligned} \tag{B1}$$

to the respective energy densities. Note that this implies that Eqs. (18) to (20) are also valid, because these equations directly follow from the ansatz for the head-to-head DW. The only difference is that they have to be evaluated using the respective DW widths, which are calculated in the following.

1. Perpendicular magnetic fields

The energy density for a uniaxial system with a magnetic field perpendicular to the nanowire is obtained by supplementing Eq. (15) with a Zeeman term and assuming that $K_x = 0$, which yields

$$\begin{aligned}\varepsilon(\Theta,\Phi) = A\left[\left(\frac{\partial\Theta}{\partial z}\right)^2+\sin^2\Theta\left(\frac{\partial\Phi}{\partial z}\right)^2\right]\\ -K_z\cos^2\Theta-\mathcal{M}B\cos\Phi\sin\Theta.\end{aligned} \tag{B2}$$

Without loss of generality we assume that the external field is in x direction and that $B > 0$. Note that magnetic fields parallel to the nanowire could also be included in the energy density. However, they lead to a constant drift of DWs [13] and since here we are only interested in their Brownian motion, we restrict the calculations to perpendicular fields. Inserting the ansatz for the head-to-head DW (B1) into the above energy density and spatial integration yields the energy of a domain wall in the presence of a perpendicular magnetic field as

$$E(\Psi,\Delta) = 2\frac{A}{\Delta}+(2K_z-\pi\mathcal{M}B\cos\Psi)\Delta+E_0, \tag{B3}$$

where E_0 is the irrelevant energy of the homogeneous state. The above expression is minimized by $\Psi = 0$ and $\Delta = \sqrt{A/(K_z-\pi\mathcal{M}B/2)}$. Harmonic expansion around this minimum yields the spring constant $\kappa = \Delta\pi\mathcal{M}B$. The angular potential energy barrier follows as $\Delta E = \pi\mathcal{M}B[\sqrt{A/(K_z+\pi\mathcal{M}B/2)}+\sqrt{A/(K_z-\pi\mathcal{M}B/2)}]$ which reduces to $\Delta E \approx 2\pi\mathcal{M}B\sqrt{A/K_z}$ for low perpendicular magnetic fields. As such, it can be easily manipulated by varying the applied field. Recalling that the ratio between thermal energy and the angular energy barrier has a crucial impact on the Brownian motion of DWs, as it determines if the dynamics are above or below the thermal Walker breakdown (see Sec. III C), we conclude that varying the perpendicular magnetic field allows for an efficient manipulation of the diffusion of DWs at a fixed temperature.

2. DMI

The energy density for a uniaxial nanowire oriented along the z axis with DMI reads [51,52]

$$\varepsilon(\Theta,\Phi) = A\left[\left(\frac{\partial\Theta}{\partial z}\right)^2 + \sin^2\Theta\left(\frac{\partial\Phi}{\partial z}\right)^2\right] - K_z\cos^2\Theta + \begin{pmatrix}\mathcal{D}^x\\ \mathcal{D}^y\\ \mathcal{D}^z\end{pmatrix}\left[\frac{\partial\Theta}{\partial z}\begin{pmatrix}-\sin\Phi\\ \cos\Phi\\ 0\end{pmatrix} - \sin\Theta\frac{\partial\Phi}{\partial z}\begin{pmatrix}\cos\Phi\cos\Theta\\ \sin\Phi\cos\Theta\\ -\sin\Theta\end{pmatrix}\right], \tag{B4}$$

with $\boldsymbol{\mathcal{D}} = (\mathcal{D}^x, \mathcal{D}^y, \mathcal{D}^z)^{\mathrm{T}}$ being the DM vector. It is convenient to choose a reference frame where one of the components of the DM vector perpendicular to the nanowire is zero. Without loss of generality we assume that $\mathcal{D}^y = 0$.

Under said assumption, the energy of a head-to-head DW described by Eq. (B1) in a uniaxial system with DMI follows from the above energy density as

$$E(\Psi,\Delta) = 2\frac{A}{\Delta} + 2K_z\Delta - \pi\mathcal{D}^x\sin\Psi + E_0. \tag{B5}$$

The contribution of the DMI to this energy only depends on the total rotation of the spins in the DW and is independent of the DW width. Since here we are considering head-to-head DWs, this total rotation amounts to π. The energy given by Eq. (B5) is minimal for $\Delta = \sqrt{A/K_z}$ and $\Psi = \mathrm{sgn}(\mathcal{D}^x)\pi/2$. Harmonic expansion around this minimum yields for the spring constant $\kappa = \pi|\mathcal{D}^x|$. The energy barrier is given by $\Delta E = 2\pi|\mathcal{D}^x|$.

Note that above a critical value of $\mathcal{D}^x_{\mathrm{c}} = 4\sqrt{A/K_z}/\pi$ the energy of the DW becomes negative and the formation of a spin spiral state [53] becomes favorable.

APPENDIX C: THE CONCEPT OF DW MASS

Our expression for the diffusion coefficient in biaxial systems with a large angular potential, Eq. (14), is in agreement with a previous study [27]. There, however, the coupling between Ψ and Z was neglected. Instead, the authors considered the following massive Langevin equation

$$m\ddot{Z} + \alpha\Gamma_Z\dot{Z} = F_Z^{\mathrm{th}} \tag{C1}$$

for the spatial dynamics of the DW. This equation can be derived from Eq. (7) by reducing the two coupled first order differential equations into one second order differential equation [15]. Note that in doing so, any time dependence of the forces is neglected. In addition, this approach fails if $\kappa = 0$. In this description the DW appears as a one-dimensional object with mass m. For Γ_Ψ and Γ_Z as given by Eq. (18), this mass corresponds to the so-called Döring mass [43] which reads

$$m = \left(\frac{2\mathcal{M}}{\gamma}\right)^2\frac{1+\alpha^2}{\kappa}. \tag{C2}$$

The massive Langevin equation (C1) is a first order differential equation of $\dot{Z}$ and hence it can be solved analogous to what is laid out in Appendix A, specifically by using Eq. (A6). The solution to Eq. (C1) is given by

$$\dot{Z}(t) = e^{-\frac{\alpha\Gamma_Z}{m}t}\dot{Z}(0) + \int_0^t e^{-\frac{\alpha\Gamma_Z}{m}(t-t')}F_z^{\mathrm{th}}(t')\,dt' \tag{C3}$$

from which it follows that

$$\langle\dot{Z}(t)\rangle = e^{-\frac{\alpha\Gamma_Z}{m}t}\,\langle\dot{Z}(0)\rangle\,, \tag{C4}$$

$$\langle\dot{Z}^2(t)\rangle = \left[\langle\dot{Z}^2(0)\rangle - \frac{k_{\mathrm{B}}T}{m}\right]e^{-2\frac{\alpha\Gamma_Z}{m}t} + \frac{k_{\mathrm{B}}T}{m}. \tag{C5}$$

The above expressions describe the convergence to thermal equilibrium, where $\langle\dot{Z}(t)\rangle = 0$ and where $\langle\dot{Z}^2(t)\rangle = k_{\mathrm{B}}T/m$, in agreement with the equipartition theorem. Since we are interested in the Brownian motion of DWs, we can assume thermal equilibrium at all times.

The displacement can be calculated by time integration of Eq. (C3), $\Delta Z(t) = \int_0^t \dot{Z}(t')\,dt'$. In thermal equilibrium we get that $\langle\Delta Z(t)\rangle = 0$ and the MSD for a DW as a massive object reads

$$\langle\Delta Z(t)^2\rangle = 2\frac{k_{\mathrm{B}}T}{\alpha\Gamma_Z}\left[t - \frac{m}{\alpha\Gamma_Z}\left(1 - e^{-\frac{\alpha\Gamma_Z}{m}t}\right)\right]. \tag{C6}$$

The nontrivial time dependence of the massive MSD can be understood in terms of a transition time $t^{\mathrm{trans}} = m/(\alpha\Gamma_Z)$ with a distinct behavior for $t \ll t^{\mathrm{trans}}$ and $t \gg t^{\mathrm{trans}}$:

$$\langle\Delta Z^2(t)\rangle = \begin{cases}\frac{k_{\mathrm{B}}T}{m}t^2, & t \ll t^{\mathrm{trans}},\\ 2\frac{k_{\mathrm{B}}T}{\alpha\Gamma_Z}t, & t \gg t^{\mathrm{trans}}.\end{cases} \tag{C7}$$

Note that the transition time as defined here coincides with the one defined in Sec. II C, since $m/(\alpha\Gamma_Z) = k_{\mathrm{B}}T/(D_\Psi^{\mathrm{uni}}\kappa)$. The result for short times describes the ballistic dynamics of a free particle, where for short times $\Delta Z(t) = \dot{Z}(0)t$ and $\langle\dot{Z}(0)^2\rangle = k_{\mathrm{B}}T/m$ in thermal equilibrium. This is different from what is obtained by the full two-variable calculation, see Eq. (11), where we obtained a linear increase of the MSD with the slope being two times the uniaxial diffusion coefficient. The long term dependence on time, however, is the same for both calculations. This is shown in Fig. 4. The MSD obtained

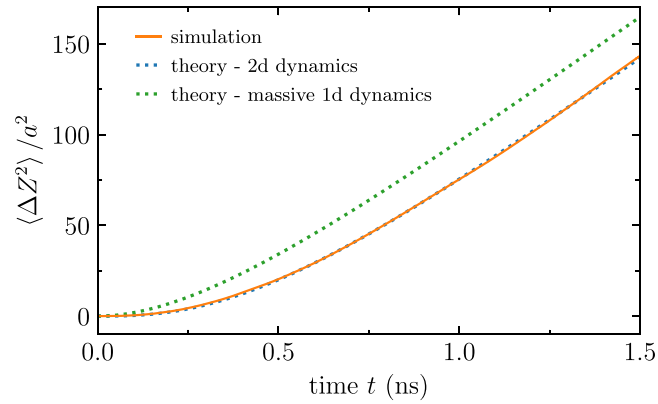

FIG. 4. Comparison of simulation results for the MSD of DWs in a biaxial system with $d_x = 0.1$ meV and for $\alpha = 0.01$ with predictions based on the full two-variable calculation (11) and the massive single-variable model (C6).

from a full two-variable calculation agrees perfectly with the simulation data, whereas the MSD obtained by the massive single-variable calculation fails to correctly describe the short term behavior, which leads to a constant offset from the simulation data in the long term limit.

While Eq. (C7) exhibits similar features as Eq. (11) (acceleration phase, linear regime in long term limit) and is in reasonable agreement with simulation results for finite κ, it is unable to capture the dynamics in uniaxial systems for which $\kappa = 0$: for $\kappa \to 0$ the mass diverges in Eq. (C6) and the acceleration phase extends to infinity. Consequently, the MSD of a massive DW in uniaxial systems is zero at all times. This is in strong contrast to our derivations in Sec. II B, which predict a small but finite diffusion coefficient (6) and the absence of an acceleration phase, in agreement with our simulations in Sec. III A. Hence we conclude that, whenever possible, the dynamics of DWs should be described by the two-dimensional equation of motion for the collective coordinates Ψ and Z, instead of the massive one-dimensional equation of motion for Z.

[1] S. S. P. Parkin, M. Hayashi, and L. Thomas, Magnetic domain-wall racetrack memory, Science **320**, 190 (2008).

[2] A. Fert, V. Cros, and J. Sampaio, Skyrmions on the track, Nat. Nanotechnol. **8**, 152 (2013).

[3] F. Jonietz, S. Mühlbauer, C. Pfleiderer, A. Neubauer, W. Münzer, A. Bauer, T. Adams, R. Georgii, P. Böni, R. A. Duine, K. Everschor, M. Garst, and A. Rosch, Spin transfer torques in MnSi at ultralow current densities, Science **330**, 1648 (2010).

[4] S. Woo, K. Litzius, B. Krüger, M.-Y. Im, L. Caretta, K. Richter, M. Mann, A. Krone, R. M. Reeve, M. Weigand, P. Agrawal, I. Lemesh, M.-A. Mawass, P. Fischer, M. Kläui, and G. S. D. Beach, Observation of room-temperature magnetic skyrmions and their current-driven dynamics in ultrathin metallic ferromagnets, Nat. Mater. **15**, 501 (2016).

[5] K. Litzius, I. Lemesh, B. Krüger, P. Bassirian, L. Caretta, K. Richter, F. Büttner, K. Sato, O. A. Tretiakov, J. Förster, R. M. Reeve, M. Weigand, I. Bykova, H. Stoll, G. Schütz, G. S. D. Beach, and M. Kläui, Skyrmion Hall effect revealed by direct time-resolved x-ray microscopy, Nat. Phys. **13**, 170 (2017).

[6] L. Caretta, M. Mann, F. Büttner, K. Ueda, B. Pfau, C. M. Günther, P. Hessing, A. Churikova, C. Klose, M. Schneider, D. Engel, C. Marcus, D. Bono, K. Bagschik, S. Eisebitt, and G. S. D. Beach, Fast current-driven domain walls and small skyrmions in a compensated ferrimagnet, Nat. Nanotechnol. **13**, 1154 (2018).

[7] L. Caretta, S.-H. Oh, T. Fakhrul, D.-K. Lee, B. H. Lee, S. K. Kim, C. A. Ross, K.-J. Lee, and G. S. D. Beach, Relativistic kinematics of a magnetic soliton, Science **370**, 1438 (2020).

[8] D. Kumar, T. Jin, R. Sbiaa, M. Kläui, S. Bedanta, S. Fukami, D. Ravelosona, S.-H. Yang, X. Liu, and S. Piramanayagam, Domain wall memory: Physics, materials, and devices, Phys. Rep. **958**, 1 (2022).

[9] W. Jiang, P. Upadhyaya, Y. Fan, J. Zhao, M. Wang, L.-T. Chang, M. Lang, K. L. Wong, M. Lewis, Y.-T. Lin, J. Tang, S. Cherepov, X. Zhou, Y. Tserkovnyak, R. N. Schwartz, and K. L. Wang, Direct Imaging of Thermally Driven Domain Wall Motion in Magnetic Insulators, Phys. Rev. Lett. **110**, 177202 (2013).

[10] S. Selzer, U. Atxitia, U. Ritzmann, D. Hinzke, and U. Nowak, Inertia-Free Thermally Driven Domain-Wall Motion in Antiferromagnets, Phys. Rev. Lett. **117**, 107201 (2016).

[11] X. Yu, F. Kagawa, S. Seki, M. Kubota, J. Masell, F. S. Yasin, K. Nakajima, M. Nakamura, M. Kawasaki, N. Nagaosa, and Y. Tokura, Real-space observations of 60-nm skyrmion dynamics in an insulating magnet under low heat flow, Nat. Commun. **12**, 5079 (2021).

[12] G. S. D. Beach, C. Nistor, C. Knutson, M. Tsoi, and J. L. Erskine, Dynamics of field-driven domain-wall propagation in ferromagnetic nanowires, Nat. Mater. **4**, 741 (2005).

[13] N. L. Schryer and L. R. Walker, The motion of 180° domain walls in uniform dc magnetic fields, J. Appl. Phys. **45**, 5406 (1974).

[14] J. C. Slonczewski, Dynamics of magnetic domain walls, AIP Conf. Proc. **5**, 170 (1972).

[15] A. Malozemoff and J. Slonczewski, V - Wall dynamics in one dimension, in *Magnetic Domain Walls in Bubble Materials*, edited by A. Malozemoff and J. Slonczewski (Academic, New York, 1979), pp. 123–143.

[16] G. Tatara and H. Kohno, Theory of Current-Driven Domain Wall Motion: Spin Transfer versus Momentum Transfer, Phys. Rev. Lett. **92**, 086601 (2004).

[17] A. Thiaville, Y. Nakatani, J. Miltat, and Y. Suzuki, Micromagnetic understanding of current-driven domain wall motion in patterned nanowires, Europhys. Lett. **69**, 990 (2005).

[18] D. Hinzke and U. Nowak, Domain Wall Motion by the Magnonic Spin Seebeck Effect, Phys. Rev. Lett. **107**, 027205 (2011).

[19] F. Schlickeiser, U. Ritzmann, D. Hinzke, and U. Nowak, Role of Entropy in Domain Wall Motion in Thermal Gradients, Phys. Rev. Lett. **113**, 097201 (2014).

[20] A. Donges, N. Grimm, F. Jakobs, S. Selzer, U. Ritzmann, U. Atxitia, and U. Nowak, Unveiling domain wall dynamics of ferrimagnets in thermal magnon currents: Competition of angular momentum transfer and entropic torque, Phys. Rev. Res. **2**, 013293 (2020).

[21] E. Martinez, L. Lopez-Diaz, L. Torres, C. Tristan, and O. Alejos, Thermal effects in domain wall motion: Micromagnetic simulations and analytical model, Phys. Rev. B **75**, 174409 (2007).

[22] J. Leliaert, B. Van de Wiele, A. Vansteenkiste, L. Laurson, G. Durin, L. Dupré, and B. Van Waeyenberge, Creep turns linear in narrow ferromagnetic nanostrips, Sci. Rep. **6**, 20472 (2016).

[23] A. A. Ivanov, V. A. Orlov, and I. N. Orlova, On the theory of the thermofluctuation motion of domain walls in nanowires, Phys. Met. Metallogr. **114**, 631 (2013).

[24] A. A. Ivanov and V. A. Orlov, On the simulation of the Brownian motion of a domain wall in nanowires, Phys. Solid State **56**, 2430 (2014).

[25] A. A. Ivanov and V. A. Orlov, Simulation of the Brownian motion of the domain wall in a nonlinear force field of nanowires, Eur. Phys. J. B **88**, 2 (2015).

[26] J. Leliaert, B. Van de Wiele, J. Vandermeulen, A. Coene, A. Vansteenkiste, L. Laurson, G. Durin, B. Van Waeyenberge, and

L. Dupré, Thermal effects on transverse domain wall dynamics in magnetic nanowires, Appl. Phys. Lett. **106**, 202401 (2015).

[27] J. Miltat, S. Rohart, and A. Thiaville, Brownian motion of magnetic domain walls and skyrmions, and their diffusion constants, Phys. Rev. B **97**, 214426 (2018).

[28] J. Zázvorka, F. Jakobs, D. Heinze, N. Keil, S. Kromin, S. Jaiswal, K. Litzius, G. Jakob, P. Virnau, D. Pinna, K. Everschor-Sitte, L. Rózsa, A. Donges, U. Nowak, and M. Kläui, Thermal skyrmion diffusion used in a reshuffler device, Nat. Nanotechnol. **14**, 658 (2019).

[29] D. Pinna, F. Abreu Araujo, J.-V. Kim, V. Cros, D. Querlioz, P. Bessiere, J. Droulez, and J. Grollier, Skyrmion Gas Manipulation for Probabilistic Computing, Phys. Rev. Appl. **9**, 064018 (2018).

[30] T. Nozaki, Y. Jibiki, M. Goto, E. Tamura, T. Nozaki, H. Kubota, A. Fukushima, S. Yuasa, and Y. Suzuki, Brownian motion of skyrmion bubbles and its control by voltage applications, Appl. Phys. Lett. **114**, 012402 (2019).

[31] M. A. Brems, M. Kläui, and P. Virnau, Circuits and excitations to enable Brownian token-based computing with skyrmions, Appl. Phys. Lett. **119**, 132405 (2021).

[32] I. Dzyaloshinsky, A thermodynamic theory of "weak" ferromagnetism of antiferromagnetics, J. Phys. Chem. Solids **4**, 241 (1958).

[33] T. Moriya, New Mechanism of Anisotropic Superexchange Interaction, Phys. Rev. Lett. **4**, 228 (1960).

[34] T. L. Gilbert, A phenomenological theory of damping in ferromagnetic materials, IEEE Trans. Magn. **40**, 3443 (2004).

[35] U. Nowak, Classical spin models, in *Handbook of Magnetism and Advanced Magnetic Materials*, edited by H. Kronmüller and S. Parkin (Wiley, New York, 2007).

[36] M. Weißenhofer and U. Nowak, Diffusion of skyrmions: The role of topology and anisotropy, New J. Phys. **22**, 103059 (2020).

[37] R. Kubo, The fluctuation-dissipation theorem, Rep. Prog. Phys. **29**, 255 (1966).

[38] C. Schütte, J. Iwasaki, A. Rosch, and N. Nagaosa, Inertia, diffusion, and dynamics of a driven skyrmion, Phys. Rev. B **90**, 174434 (2014).

[39] N. Kerber, M. Weißenhofer, K. Raab, K. Litzius, J. Zázvorka, U. Nowak, and M. Kläui, Anisotropic skyrmion diffusion controlled by magnetic-field-induced symmetry breaking, Phys. Rev. Appl. **15**, 044029 (2021).

[40] M. Weißenhofer, L. Rózsa, and U. Nowak, Skyrmion Dynamics at Finite Temperatures: Beyond Thiele's Equation, Phys. Rev. Lett. **127**, 047203 (2021).

[41] L. Zhao, Z. Wang, X. Zhang, X. Liang, J. Xia, K. Wu, H.-A. Zhou, Y. Dong, G. Yu, K. L. Wang, X. Liu, Y. Zhou, and W. Jiang, Topology-Dependent Brownian Gyromotion of a Single Skyrmion, Phys. Rev. Lett. **125**, 027206 (2020).

[42] B. Øksendal, *Stochastic Differential Equations: An Introduction with Applications*, Vol. 82 (Springer-Verlag, Berlin, Heidelberg, 2000).

[43] W. Döring, Über die Trägheit der Wände zwischen Weißschen Bezirken, Z. Naturforschung A **3**, 373 (1948).

[44] P. Hänggi, P. Talkner, and M. Borkovec, Reaction-rate theory: Fifty years after Kramers, Rev. Mod. Phys. **62**, 251 (1990).

[45] S. Lifson and J. L. Jackson, On the self-diffusion of ions in a polyelectrolyte solution, J. Chem. Phys. **36**, 2410 (1962).

[46] S. Tyablikov, Retarded and advanced green functions in the theory of ferromagnetism, Ukr. Mat. Zh. **11**, 287 (1959).

[47] H. Callen and E. Callen, The present status of the temperature dependence of magnetocrystalline anisotropy, and the l(l+1)2 power law, J. Phys. Chem. Solids **27**, 1271 (1966).

[48] M. Hayashi, L. Thomas, C. Rettner, R. Moriya, Y. B. Bazaliy, and S. S. P. Parkin, Current Driven Domain Wall Velocities Exceeding the Spin Angular Momentum Transfer Rate in Permalloy Nanowires, Phys. Rev. Lett. **98**, 037204 (2007).

[49] L. F. Yin, D. H. Wei, N. Lei, L. H. Zhou, C. S. Tian, G. S. Dong, X. F. Jin, L. P. Guo, Q. J. Jia, and R. Q. Wu, Magnetocrystalline Anisotropy in Permalloy Revisited, Phys. Rev. Lett. **97**, 067203 (2006).

[50] R. Durrett, *Probability: Theory and Examples* (Cambridge University Press, Cambridge, 2019), Vol. 49.

[51] M. Heide, G. Bihlmayer, and S. Blügel, Dzyaloshinskii-Moriya interaction accounting for the orientation of magnetic domains in ultrathin films: Fe/W(110), Phys. Rev. B **78**, 140403(R) (2008).

[52] T. Conzelmann, S. Selzer, and U. Nowak, Domain walls in antiferromagnets: The effect of Dzyaloshinskii-Moriya interactions, J. Appl. Phys. **127**, 223908 (2020).

[53] M. Bode, M. Heide, K. von Bergmann, P. Ferriani, S. Heinze, G. Bihlmayer, A. Kubetzka, O. Pietzsch, S. Blügel, and R. Wiesendanger, Chiral magnetic order at surfaces driven by inversion asymmetry, Nature (London) **447**, 190 (2007).